Copyright Warning & Restrictions

The copyright law of the United States (Title 17, United States Code) governs the making of photocopies or other reproductions of copyrighted material.

Under certain conditions specified in the law, libraries and archives are authorized to furnish a photocopy or other reproduction. One of these specified conditions is that the photocopy or reproduction is not to be "used for any purpose other than private study, scholarship, or research." If a, user makes a request for, or later uses, a photocopy or reproduction for purposes in excess of "fair use" that user may be liable for copyright infringement,

This institution reserves the right to refuse to accept a copying order if, in its judgment, fulfillment of the order would involve violation of copyright law.

Please Note: The author retains the copyright while the New Jersey Institute of Technology reserves the right to distribute this thesis or dissertation

Printing note: If you do not wish to print this page, then select "Pages from: first page # to: last page #" on the print dialog screen

NJIT
New Jersey's Science & Technology University

The Van Houten library has removed some of the personal information and all signatures from the approval page and biographical sketches of theses and dissertations in order to protect the identity of NJIT graduates and faculty.

ABSTRACT

MEASUREMENT OF THE HALL COEFFICIENT AND ELECTRON MOBILITY USING VAN DER PAUW TYPE HALL EFFECT MEASUREMENTS

by
Hong-Sheng Luo

Hall effect measurement in the electrical characterization of semiconductor materials is very important. We set up the Hall effect measurement system and examined the system with a standard sample. The experimental results show that this Hall measurement system worked as well as expected. We also used this system to study the GaAs/GaAs and InGaAs/GaAs which grown by MBE. Finally, we disscussed and consided some common problems of Hall measurement. Some useful formulas and plots are presented.

MEASUREMENT OF THE HALL COEFFICIENT AND ELECTRON MOBILITY USING VAN DER PAUW TYPE HALL EFFECT MEASUREMENTS

by
Hong-Sheng Luo

ROBERT W. VAN HOUTEN LIBRARY
NEW JERSEY INSTITUTE OF TECHNOLOGY

A Thesis
Submitted to the Faculty of
New Jersey Institute of Technology
in Partial Fulfillment of the Requirements for the Degree of
Master of Science in Applied Physics

Department of Physics

October 1994

APPROVAL PAGE

MEASUREMENT OF THE HALL COEFFICIENT AND ELECTRON MOBILITY USING VAN DER PAUW TYPE HALL EFFECT MEASUREMENTS

Hong-Sheng Luo

Dr. Ken K. Chin, Thesis Advisor Date
Professor
Department of Physics
New Jersey Institute of Technology

Dr. J. C. Hensel, Committee Member Date
Distinguished Research Professor
Department of Physics
New Jersey Institute Technology

Dr. Yuan Yan, Committee Member Date
Visiting Professor
Department of Physics
New Jersey Institute of Technology

BIOGRAPHICAL SKETCH

Author: Hong-Sheng Luo

Degree: Master of Science in Applied Physics

Date: October 1994

Undergraduate and Graduate Education:

- Master of Applied Physics
  New Jersey Institute of Technology, Newark, NJ, 1994
- Bachelor of Science in Physics
  Langzhong University, Langzhong, P.R.China, 1984

Major: Applied Physics

This thesis is dedicated to
my parents

ACKNOWLEDGMENT

The author would like to express his gratitude to his advisor Dr. K. Ken Chin for his support, guidance and great help during the thesis research.

The author would also like to thank Dr. J. C. Hensel for his helpful dis cussions in the research and for his guidance in the use of measurement apparatus.

Special thanks to Professor Yuan Yan for serving as a member of the committee and giving me very helpful suggestions on the thesis.

The author would also like to thank Professor Guanhua Feng for supplying me the high quality standard sample. The author has gotten a lot of help during his study and research work from many people in his group. The author wishes to thank all of them.

TABLE OF CONTENTS

Chapter	Page
1 INTRODUCTION	1
1.1 The Hall Effect and Electrical conductivity	1
1.2 The Significance of the Hall Effect	2
1.3 The Application of the InGaAs/GaAs System	3
1.4 The Objective of the Thesis	4
2 PRINCIPLE OF HALL EFFECT AND VAN DER PAUW THEORY	5
2.1 Electrical Conductivity and the Hall Effect	5
2.2 Collinear Four-probe Resistivity Measurement	15
2.3 Van Der Pauw Theory	18
2.4 Systematic Errors	22
3 EXPERIMENTAL PROCEDURES AND SET-UP	27
3.1 Measurement Procedures	27
3.2 Van Der Pauw Configuration	30
3.3 Experimental Set-up of Hall Measurement	32
3.4 Ohmic Contact	33
4 HALL MEASUREMENT RESULT AND DISCUSSION	35
4.1 Equipment System of Hall Measurement	35
4.2 Experiment of Hall Effect	36
4.3 Result and Discussion	37
5 CONCLUSION	39
REFERENCES	40

LIST OF TABLES

Table **Page**

2.1 Permutations of current and Magnetic Field for Hall Measurement................25

3.1 Units of Measurement..25

3.2 Ohmic Contact Technology for III-V Conpound Semiconductors...................34

4.1 The Range and Precision of the equipment...35

4.2 Experiment Result of the Sample...37

4.3 Comparison of Sampling and Standard Hall Measurement............................37

LIST OF FIGURES

Figure		Page
1	The Hall Effect	1
2	Schematic Representation of Wafer in which Electrons are the Dominate Charge Carriers.	6
3	The Hall Effect in a Rectangular Plat in which Electrons and Hole are Charge Carriers.	12
4	A Standard Hall-Bar Configuration	13
5	Collinear Four-probe Array on a Semi-infinite Sheet	15
6	The Figure of the Deriving equation for Four-probe Method	16
7	Square Four-probe array on a Semi-infinite surface	18
8	Representation of a Semi-Infinite Half-Plane	19
9	The Function f Used to Determine the Specific Resistivity of a Specimen	22
10	Hall Effect and Principal Thermomagetic Effect Shown with Their Orientation in Cartesian Coordinates	23
11	External Comensation Circuits for Eliminating the Misalignment Potential Between Hall Electrodes	29
12	Four Common Patterns Used for Van Der Pauw Resistivity and Hall Effect	31

CHAPTER 1

INTRODUCTION

1.1 The Hall Effect and Electrical Conductivity

In view of the important part played by the Hall effect in the study of the conduction process, a few introductory remarks will be made concerning it and its relation to the electrical conductivity. This effect was discovered by E.H.Hall in 1879 [1] during an investigation of the nature of the force acting on a conductor carrying a current in a magnetic field. Hall found that as show in Figure 1. The Hall coefficient R is defined by the equation

$$E_y = RJ_xB_z \qquad (1.1)$$

This defination will be considered more precisely in Chapter 2. By involving Lorentz force, it is verified that the Hall coefficient defined by equation (1.1) is inversely proportional to the concentration of conducting electrical charge carries:

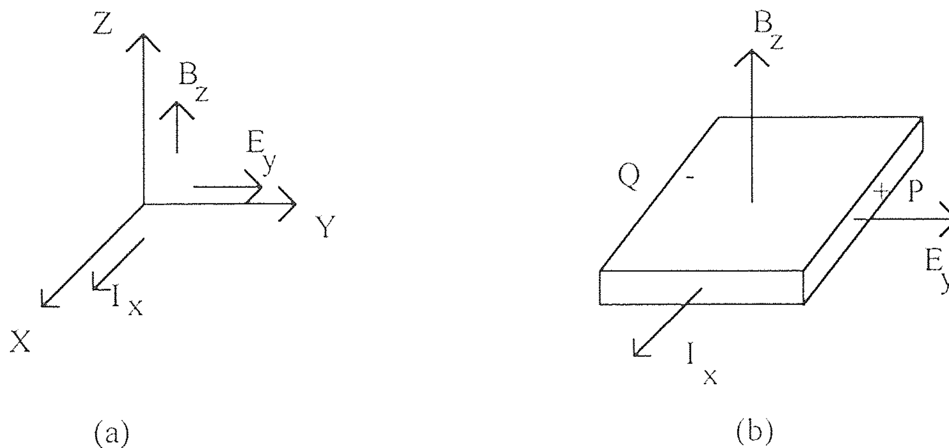

Figure 1. The Hall effect. (a) Relative direction of current, magnetic induction and Hall field for negative electrons. (b) Strip of conducting material: edges parallel to x and y directions. Points P and Q are at opposite ends of an equipotential in the absence of a magnetic field. When induction B_z is applied , P has a positive potential relative to Q (for negative electrons).

$$R = \frac{1}{nq} \tag{1.2}$$

The convention is adopted that when q is negative R is taken as negative.

A few words must also be said about the electrical conductivity σ. This may be defined by writing

$$\sigma = nq\mu \tag{1.3}$$

where μ is the electron mobility. This must be within the validity of Ohm's law, independent of E. Equation (1.3) shows that the interpretation of measurements of conductivity is not so straightforward as that of the Hall effect, but the combination of the two yields that very informative quantity, the mobility . From (1.2) and (1.3),

$$|R|\,\sigma = \mu \tag{1.4}$$

When the mobility are considered in more detail it will be found that a numerical factor enters into (1.4), as in (1.2).

1.2 The Significance of the Hall Effect

It is because of the simple relation (1.2) between the Hall coefficient and the electron concentration that measurement of the Hall coefficient is very useful in the study of conduction processes. It is a matter worthy of note that when Hall did his pioneering research and the Hall effect, the negatively charged electron had not been discovered yet, and it was assumed that the conducting carriers were positively charged. A more exact general derivation of equation (1.2) will be given in Chapter 2.

The study of the simple transport properties can make a useful contribution to solid state physics for three reasons. In the first place, the conductivity and Hall effect can be measured on any solid, but the elegant experiments just described can only be carried out when very exacting conditions are satisfied . We have seen

how the simple experiments were the first to indicate the fundamental correctness of the modern concepts of the solid state. They now are useful in assessing the properties of new materials not yet available in such a perfect form as silicon or germanium. The second reason is that Hall effect studies give a direct indication of the degree of purity of any semi-conductor as tools for studying the properties of impurities. The final reason is that the band structure built up is essentially the empty house in which the electrons live. We now understand a lot about the structure of the house but there is a great deal we don't know about the behavior of the electrons when they are at home .

The mechanism of collisions and scattering processes is still not completely understood. Study of the transport properties affords one of the most direct ways of investigating these processes.

1.3 The Application of the $In_xGa_{1-x}As/GaAs$ System

In recent years the growth of $In_xGa_{1-x}As$ on GaAs by molecular beam epitaxy (MBE) has attracted considerable interest. This is because MBE offers the ability to produce very thin layers, smooth surfaces, atomically abrupt interfaces, and controlled compositional and doping profiles. The reason is also potential applications for fast detectors, due to the high mobility and as light sources in the infrared region[2] and integrated optoelectronic devices with highly matured GaAs technology[3]. High-speed devices can also be achieved because the low-field mobility of $In_xGa_{1-x}As$ is higher than of GaAs and it increases with increasing indium composition[4]. Studies of such heterostructure have included observations of In content and growth parameters, mechanisms for In incorporation, segregation effects, and the electron transport properties[5]. Except for InAs on GaAs, most previous experiments concentrated on the studies of material qualities of the main work concerning the $In_xGa_{1-x}As/GaAs$ system with x values up to 0.5[6,7], As for

the study of transport properties, only a few experimental or theoretical investigations on the InGaAs/GaAs system have been reported[4,8,9]. It was found that in a highly mismatched system, dislocation scattoring becomes important in the low-temperature range and the assumption that large lattice mismatch generates higher dislocation density seems natural[4]. However , a study of the $In_xGa_{1-x}As/GaAs$ system which covered the entire indium composition range (from x=0 to 1) and utilized double-crystal x-ray diffraction (DXRD) and crossectional transmission electron microscope (XTEM) had found that, although the $In_xGa_{1-x}As$ material qualities degraded as x increased from 0 to 0.5, the material qualities recovered when x increased from 0.5 to 1 in spite of the increase in lattice mismatch[10]. So, it was suggested that lattice mismatch is not the only factor determining the epilayer qualities.

1.4 The Objective of the Thesis

We studied GaAs and $In_xGa_{1-x}As$ layers grown both on semi-insulating (SI) GaAs substrate by MBE for the x=0.5, The electron mobility and electron concentration were determial from the Hall effect measured by the Van der Pauw technique. We set up the van der Pauw-type Hall effect measurement system and tested the system which was found working well. We used a standard sample which is GaAs on SI-GaAs substrate to examine the system and investigate the $In_xGa_{1-x}As$ grown on GaAs by MBE.

CHAPTER 2

THE PRINCIPLE OF HALL EFFECT AND VAN DER PAUW THEORY

2.1 Electrical Conductivity and The Hall Effect

Some indication of the physical significance of these effects has already been given in Chapter 1. To give precise definitions the conditions of measurement must be defined. It will be assumed that the conditions are isothermal , that is to say, that no temperature gradients exist in the samples being studied. It is also possible to specify other thermal conditions, and this will be considered in the discussion of the themo-magnetic effect, but isothermal conditions are usually assumed in studying these effects.

Electrons, considered as charged particles, drift opposite to the direction of an electric field **E** with a velocity **v** driven by the force $\mathbf{F}_c = -e\mathbf{E}$, where e is 1.6×10^{-19} C. In the presence of a transverse magnetic field **B** the drifting electrons are subjected to the Lorentz force $\mathbf{F}_m = -e(\mathbf{v}\times\mathbf{B})$ and some of the electrons are deflected in a direction orthogonal to both the electric and magnetic field vectors producing a Hall field E_h which compensates the Lorenz forces

$$\mathbf{F} = -e(\mathbf{E} + \mathbf{v} \times \mathbf{B}) \qquad (2.1)$$

This acts on the electrons and produces, the two complementary galvanmagnetic phenomena, the Hall effect and the transverse magnetoresistance. In a rectangular plate such as that shown in Fig. 2 the Hall field $E_h = E_y$ compensates the y-component of the force **F**. Defining the electron mobility $\mu = ev/\mathbf{F}$ the components of the velocity vector v of the electrons are

$$\begin{aligned} v_x &= -\mu(E_x + v_y B) \\ v_y &= -\mu(E_y - v_x B) \qquad (2.2) \\ v_z &= -\mu E_z = 0 \end{aligned}$$

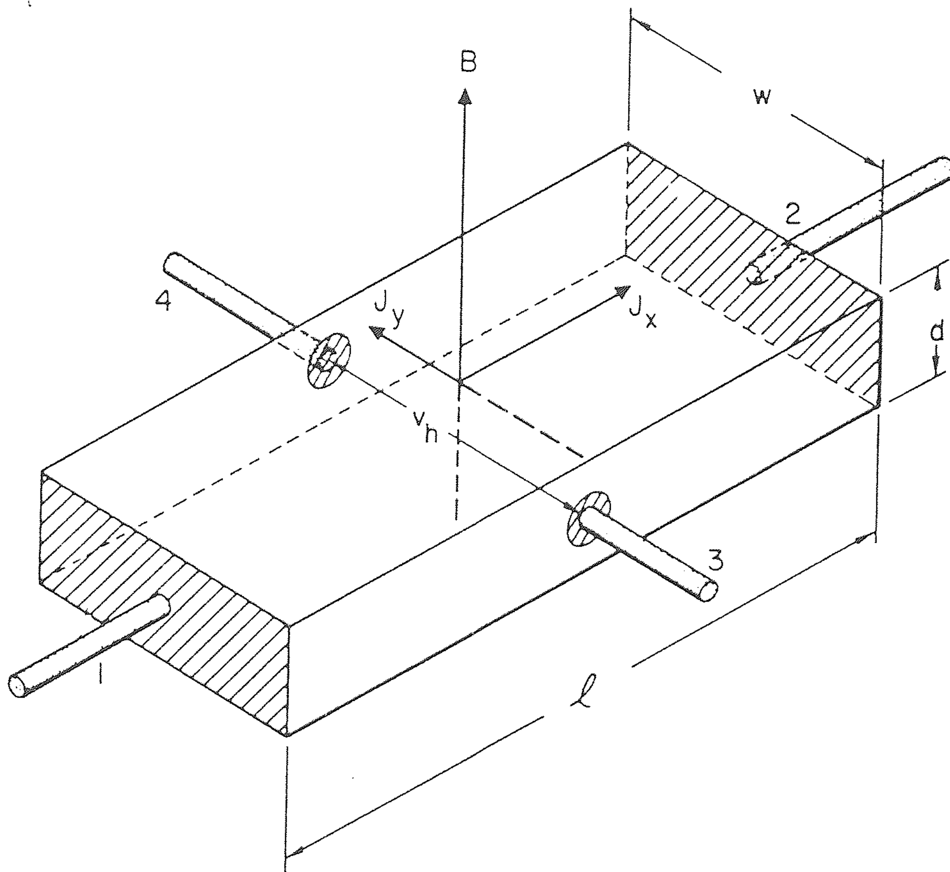

Figure 2 Schematic representation of wafer in which electrons are the dominate charge carriers. Broad area faces, wd are current contacts designated by numerals 1 and 2. Hall voltage contacts transverse to magnetic field B and current density J_x are designated 3 and 4.

Ohm's Law $\mathbf{J} = \sigma\mathbf{E}$ defines the linear relation between $\mathbf{E}$ and the current density vector $\mathbf{J} = ne\mathbf{v}$ in terms of the density of electrons n crossing a unit surface area which is perpendicular to their velocity vector in terms of Eq.(2.2). The components of $\mathbf{J}$ are

$$J_x = nev_x = \sigma\left(\frac{E_x - \mu BE_y}{1 + \mu^2 B^2}\right) \qquad J_y = nev_y = \sigma\left(\frac{E_y + \mu BE_x}{1 + \mu^2 B^2}\right) \tag{2.3}$$

When B = 0 the conductivity σ and the resistivity ρ of a homogeneous isotropic solid are scalar quantities; for $B \neq 0$ these parameters become second order tensors, $\mathbf{J} = \hat{\sigma}\mathbf{E}$ and $\mathbf{E} = \hat{\rho}\mathbf{J}$, with the cap symbol representing a tensor. Neglecting higher order terms the Ohm-Hall equations can be expessed as

$$\mathbf{E} = \rho\mathbf{J} - R_h(\mathbf{J} \times \mathbf{B}) \qquad \mathbf{J} = \sigma\mathbf{E} - \sigma R_h(\mathbf{J} \times \mathbf{B}) \tag{2.4}$$

where R_h is the coefficient of proportionality between the Hall field and the vector cross-product ($\mathbf{J} \times \mathbf{B}$). The conductivity tensor is

$$\hat{\sigma} = \begin{vmatrix} \sigma_{11} & \sigma_{12} \\ -\sigma_{12} & \sigma_{11} \end{vmatrix} = \begin{vmatrix} \dfrac{\rho}{\rho^2 + R^2{}_h B^2} & \dfrac{R_h B}{\rho^2 + R_h{}^2 B^2} \\ \dfrac{-R_h B}{\rho^2 + R^2{}_h B^2} & \dfrac{\rho}{\rho^2 + R^2{}_h B^2} \end{vmatrix} \tag{2.5}$$

It is apparent from Eq. (2.5) that all transverse elements of the "conductivity" are proportional to B and exhibit symmetry $\sigma_{ij} = -\sigma_{ji}$; in accordance with the Onsager relations, $\rho_{ij}(\mathbf{B}) = \rho_{ji}(-\mathbf{B})$ [11].

The conductivity tensor is the reciprocal of the resistivity tensor; however, the elements of the resistivity tensor are not reciprocals of the conductivity tensor. If the specimen illustrated in Fig. 2 is characterized by the scalar conductivity $\sigma = ne\mu$ then, from Eq. (2.3) for $J_y = 0$

$$-E_y = \mu BE_x \qquad v_x = \mu E_x \tag{2.6}$$

Introducing Ohm's law into Eq. (2.6) leads to

$$E_y = -R_h J_x B \tag{2.7}$$

In zero magnetic field the current streamlines are perpendicular to the equipotential planes. In a transverse magnetic field the current streamlines are rotated with respect to the equipotential planes by an angle θ defined as the Hall angle whose tangent, for $J_y = 0$, is $\tan\theta = -E_y/E_x$ hence $\tan\theta = -\sigma R_h B$.

To first order, in low or moderate magnetic fields, a Hall voltage v_h is generated between terminals 3 and 4 of Fig. 2 for an input current i applied between electrodes 1 and 2 and a transverse magnetic field B along the thickness d of the plate

$$V_h = \int_0^W E_y dy = -R_h (iB/d) \tag{2.8}$$

For electrons the Hall coefficient is inversely proportional to the electron density, $R_h = -1/ne$. Therefore μ and n can be determined quantitatively from Hall and conductivity measurements.

The magnetoresistance effect in a homogenous isotropic material in which electrons are the charge carriers may be attributed to either a complete or a partial short circuit of the Hall field E_y. From Eq. (2.3) if $E_y = 0$ then the magnetic field-dependent resistivity $\rho(B) = E_x/J_x$ and the Hall current J_y are

$$\rho(B) = \rho(0)\,(1+\mu^2 B^2), \qquad J_y/J_x = \mu B \tag{2.9}$$

where the scalar resistivity $\rho(0) = 1/\sigma$, and the magnetoresistance $\Delta\rho/\rho_0$ has a quadratic dependence on B,

$$\Delta\rho/\rho_0 = \mu^2 B^2 \tag{2.10}$$

A partial short-circuit of E_y which allows a fractional Hall current to flow in a rectangular wafer produces in it a magnetorestance which alters the linear relation expressed in Eq. (2.8) between V_h and B. Conversely, an incomplete short circuit of the Hall field, E_y reduces $\Delta\rho/\rho_0$ effective for a given B and may alter its

quadratic dependence on B expressed in Eq. (2.10). Intuitively, it is to be expected that the geometrical aspect of a wafer used for Hall effect or for magnetoresistance measurements will affect the distribution of the equipotential planes in it. For rectangular plates such as shown in Fig. 2 the length to width ratio should be equal to or greater than 3 in order to minimize the electrostatic shorting effect of its electrodes.

If charge carriers are present in more than one conduction band then the total current density **J** in a material is the vector sum of the current densities of each band and

$$\hat{\sigma} = \sum_{i=1}^{n} \hat{\sigma}_i \tag{2.11}$$

where $\hat{\sigma}_i$ is the conductivity tensor of the i th conduction band. For two conduction bands, i = 1, 2, the resistivity tensor $\hat{\rho} = 1/\hat{\sigma} = (\hat{\sigma}_1 + \hat{\sigma}_2)^{-1}$. The tensor components of a two-band system are, therefore,

$$\hat{\rho} = \begin{vmatrix} \frac{\alpha}{\alpha^2+\beta^2} & -\frac{\beta}{\alpha^2+\beta^2} \\ \frac{\beta}{\alpha^2+\beta^2} & \frac{\alpha}{\alpha^2+\beta^2} \end{vmatrix} \tag{2.12}$$

where $\alpha = \sigma_1^{11} + \sigma_2^{11}$ and $\beta = \sigma_1^{12} + \sigma_2^{12}$. Equation (2.2) is applicable to the two-band tensor as well; however the tensor components are then $\rho = \alpha \cdot \left[\alpha^2 + \beta^2\right]^{-1}$ and $R_h B = \beta \cdot \left[\alpha^2 + \beta^2\right]^{-1}$. The elements of the conductivity tensor can be expressed in terms of Eq. (2.3) for each band, i.e. , $\sigma_1, \sigma_2, R_{h_1}$ and R_{h_2}. The conductivity due to both conduction bands [12] is

$$\sigma = \frac{(\sigma_1+\sigma_2)^2 + B^2\sigma_1{}^2\sigma_2{}^2(R_{h_1}+R_{h_2})^2}{(\sigma_1+\sigma_2) + B^2\sigma_1\sigma_2(\sigma_1 R_{h_1}{}^2 + \sigma_2 R_{h_2}{}^2)} \tag{2.13}$$

and the Hall coefficient of the two-band system is

$$R_h = \frac{\sigma_1{}^2 R_{h_1} + \sigma_2{}^2 R_{h_2} + B^2\sigma_1{}^2\sigma_2{}^2 R_{h_1}R_{h_2}(R_{h_1}+R_{h_2})}{(\sigma_1+\sigma_2)^2 + B^2\sigma_1{}^2\sigma_2{}^2(R_{h_1}+R_{h_2})^2} \tag{2.14}$$

In consequence of two-band conduction Eq. (2.14) indicates that both the Hall coefficient and the conductivity become dependent on the magnetic field even if these parameters in their separate conduction bands are independent of B.

In a weak magnetic field, such that the terms multiplied by B^2 in Eqs. (2.13) and (2.14) are negligible, the conductivity and Hall coefficient approach the low field limit

$$\sigma_0 = \sigma_1 + \sigma_2 \qquad R_{h_0} = \frac{\sigma_1{}^2 R_{h_1} + \sigma_2{}^2 R_{h_2}}{(\sigma_1+\sigma_2)^2} \tag{2.15}$$

For two-band conduction in which electrons and holes are the charge carriers, Eq. (2.15) can be expressed as

$$\sigma_0 = e(n\mu_n + p\mu_p) \qquad R_{h_0} = -\frac{1}{e}\cdot\frac{n\mu_n{}^2 - p\mu_p{}^2}{(n\mu_n + p\mu_p)^2} \tag{2.16}$$

where n and p are the electron and hole densities per unit volume and μ_n and μ_p are, respectively, the electron and hole mobility. By defining the ratio of their mobility as $b = \mu_n/\mu_p$ and that of the carrier concentrations as $c = n/p$ [13] the magnetic field-dependent Hall coefficient is

$$R_h = R_{h_0}\cdot\frac{1 - X\mu_n{}^2 B^2}{1 + Y\mu_n{}^2 B^2} \tag{2.17}$$

$$X = \frac{1-c}{b^2 c-1}, \qquad Y = \frac{1-c}{1+bc}$$

The Hall angles for each band and corresponding vector diagram of the current densities are represented in Fig. 3. A magnetic field dependence of R_h or σ measured experimentally should not be considered as definitive proof of multi-band conduction. Inhomogeneities in a specimen can also give rise to $R_h(B)$ and σ (B) and can lead to erroneous conclusions unless corroborative evidence is available that the specimen is isotropic and homogenous.

When a system of electrons in equilibrium is perturbed by the application of electric and magnetic fields, collision forces will attempt to restore the system to equilibrium. For many types of such collisions, this restoration will be exponential in nature with a characteristic time constant τ, the "relaxation time ", Then, in simple isotropic systems, the current densities set up by fields will be given by

$$J_x = \sigma_{xx} E_x + \sigma_{xy} E_y \tag{2.18}$$

$$J_y = \sigma_{yx} E_x + \sigma_{yy} E_y \tag{2.19}$$

Where E_x and E_y are the electric field components, and , for an n-type sample

$$\sigma_{xx} = \sigma_{yy} = \frac{ne^2}{m^*}\left\langle \frac{\tau}{1+\omega_c^2 \tau^2} \right\rangle \tag{2.20}$$

$$\sigma_{xy} = -\sigma_{yx} = -\frac{ne^2}{m^*}\left\langle \frac{\omega_c \tau^2}{1+\omega_c^2 \tau^2} \right\rangle \tag{2.21}$$

Where $\omega_c \equiv eB/m^*$ is the cyclotron frequency and the other symbol have their usual meanings. We can define the quantities of interest for this thesis: the Hall coefficient , R_h , the Hall mobility, μ_h.

The Hall coefficient is measured in a prototype structure such as that shown in Fig. 4, the "Hall bar". This structure is long and narrow , and the voltage contacts to measure V_c and V_h , are placed far from the large-area current contacts.

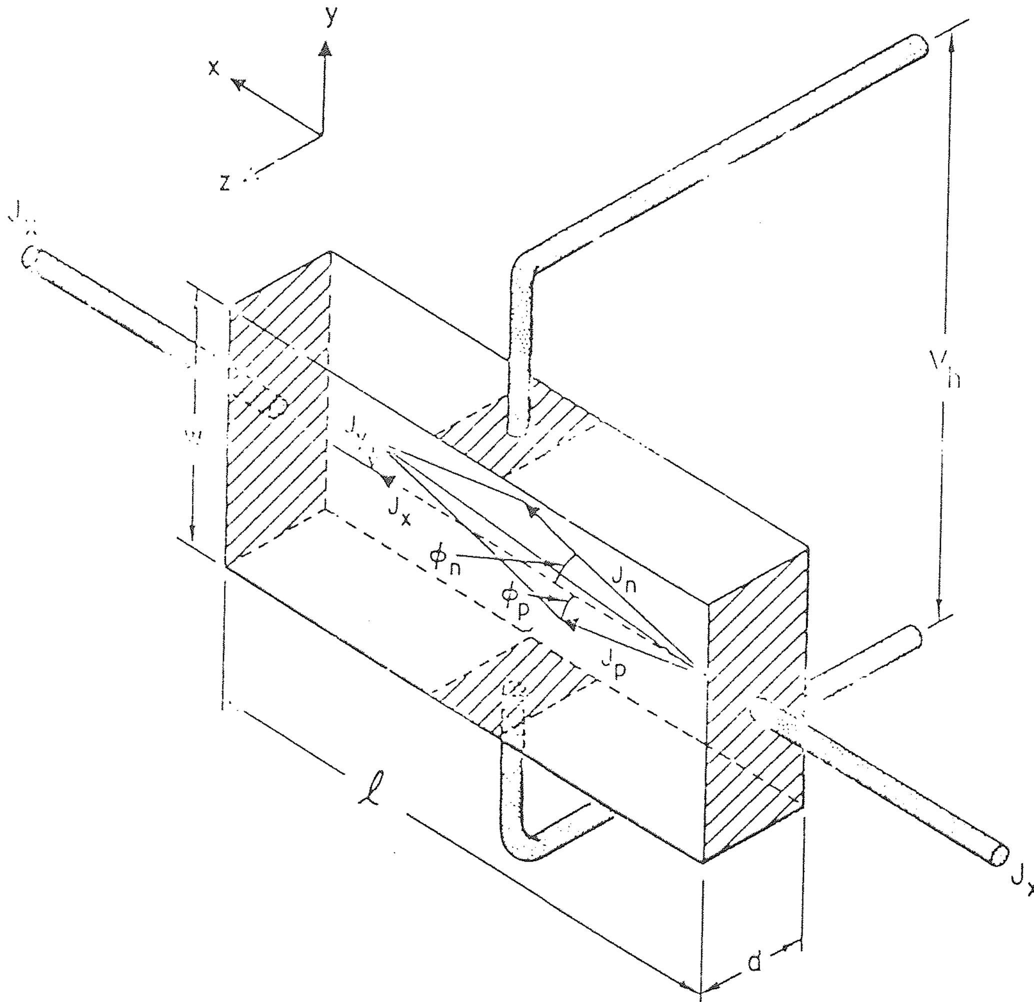

Figure 3 The Hall effect in a rectangular plate in which electrons and holes are charge carriers. The magnetic field is oriented along z-axis. The vector diagram shows longitudinal electron and hole current densities J_n and J_p and the Hall current density J_y. The corresponding Hall angles are Φ_n and Φ_p.

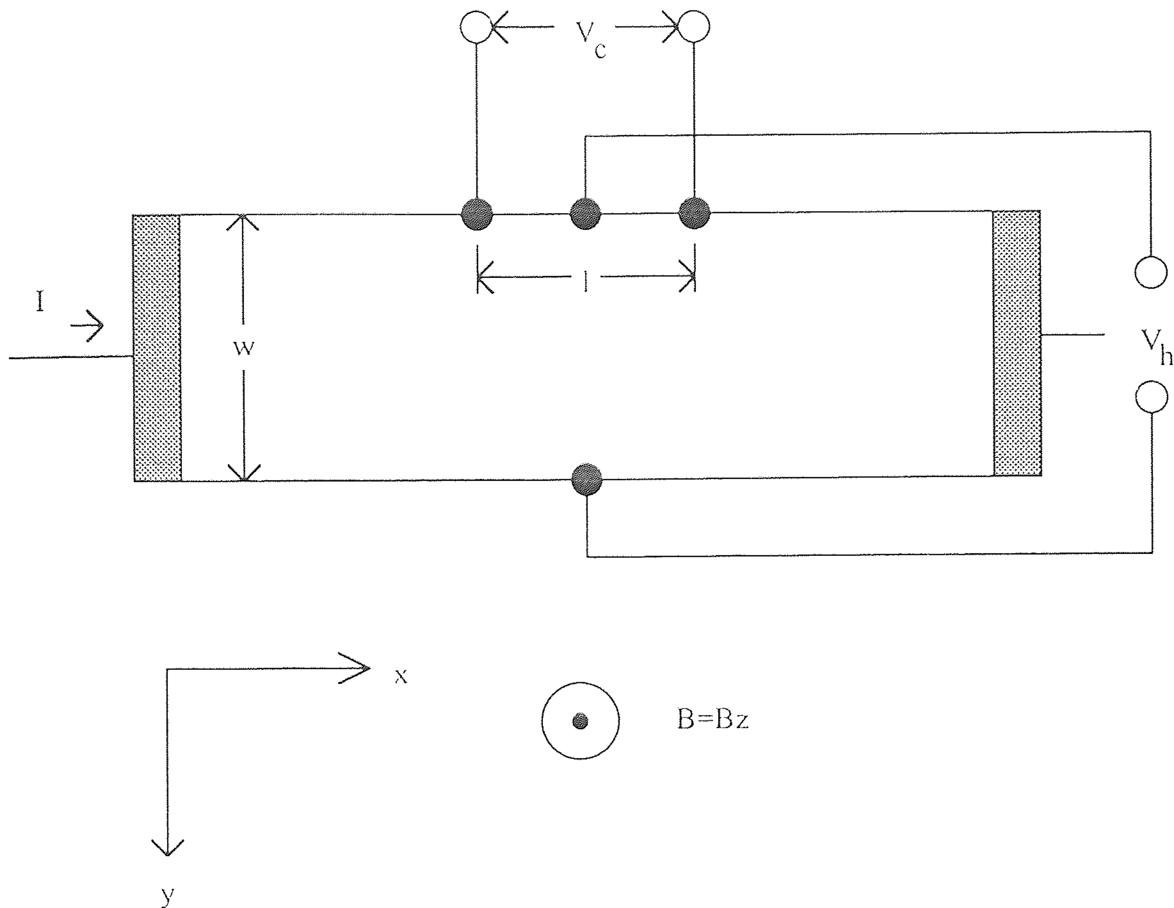

Figure 4 A standard Hall-bar configuration.

Because the voltage contacts do not carry current, $J_y = 0$. The Hall coefficient is then defined as

$$R_h \equiv \left.\frac{E_y}{J_x B}\right|_{J_y=0} = \frac{1}{B}\frac{\sigma_{xy}}{\sigma_{xx}^2 + \sigma_{xy}^2} \tag{2.22}$$

At B=0,

$$R_h = -\frac{1}{ne}\frac{\langle \tau^2 \rangle}{\langle \tau \rangle^2} \equiv -\frac{r}{ne} \equiv -\frac{1}{n_h e} \tag{2.23}$$

where r is the "Hall factor" and n is the "Hall concentration," the concentration actually measured in a Hall experiment. The quantity r (typically close to unity)

usually must be calculated by fitting μ_h vs. T to a theoretical scattering formula made up of all contribution to the scattering.

To determine the Hall mobility μ_h, we must also perform a conductivity experiment

$$J_x\Big|_{\substack{J_y=0\\B=0}} = \frac{\sigma_{xx}^2+\sigma_{xy}^2}{\sigma_{xx}}E_x\Big|_{B=0} = \sigma_{xx}E_x = \frac{ne^2\langle\tau\rangle}{m^*}E_x = ne\mu E_x \tag{2.24}$$

where $\mu \equiv e\langle\tau\rangle/m^*$ is known as the "conductivity mobility." The Hall mobility is now defined as

$$\mu_h \equiv R_h\sigma = -\frac{r}{ne}ne\mu = -r\mu \tag{2.25}$$

With respect to the symbols in Fig. 4, we calculate n and μ, along with the resistivity ρ, in laboratory units as

$$\rho = \frac{\omega d}{\ell}\frac{V_c}{I} \tag{2.26}$$

$$\mu_h = \frac{10^8}{B(\text{gauss})}\frac{V_h}{V_c}\frac{l}{\omega}\frac{cm^2}{V\text{-}s} \tag{2.27}$$

$$n_h = 6.25\times10^{10}\frac{I(\text{amp})B(\text{gauss})}{V_h(\text{volts})d(\text{cm})}\text{cm}^{-3} \tag{2.28}$$

where d is the sample thickness. Equation (2.27) and (2.28) are strictly true only for $[\mu(m^2/V\text{-}s)B(T)]^2 << 1$ or $[\mu(cm^2/V\text{-}s)B(G)]^2 << 10^{16}$, if the electrons are nondegenerate. Typically, $B\approx5\times10^3$G, so that low-B conditions are applicable as long as $\mu \leq 2\times10^4$ cm²/ V-s. Even for higher values of μB, Eq. (2.27) and (2.28) are often a good approximation.

2.2 Collinear Four-probe Resistivity Measurement

The collinear four-probe array method provides for the resistivity of specimens having a wide variety of shapes, including those having irregular boundaries and also of the resistivity of smaller regions included in a matrix with different electrical properties. Figure 3 shows four pointed equispaced probes in contact with a plane surface of a uniform isotropic material to be measured.

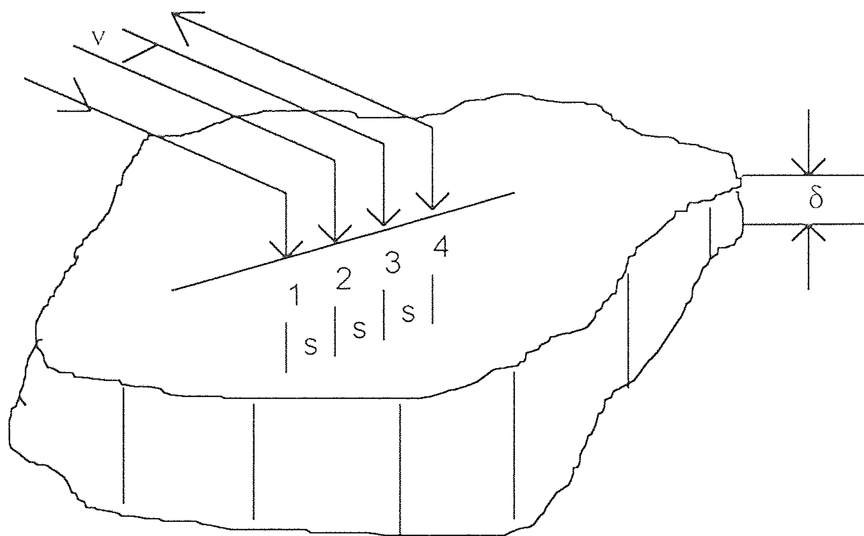

Figure 5 Collinear four-probe array on a semi-infinite sheet of thickness, δ; outer probes 1 and 4 are the current input and output probes, inner probes 2 and 3 measure the potential difference, V, between them.

The probes are considered to be far from any of the other boundaries of the specimen so that it may be considered to be an infinite area of uniform resistivity. Further constraints are:

(a) the diameter of the contact between each probe and the specimen surface should be small with respect to the distance, s, between the probes,

(b) the surface should have a high recombination rate so that any electrons and holes injected by the probes recombine in their immediate vicinity and their effect on the conductivity is negligible, and

(c) the boundary between the current-carrying electrodes and the bulk material is small in diameter and hemispherical in shape.

Let a current , i, be impressed on the two outer probes (1 and 4) with a diameter of 2α while the potential difference, V, is measured between the inner probes (2 and 3) as showen on Fig.6. When the thickness of the sample is much greater than the distance between the probes, or $\delta >> s$, the current streamlines are considered to have radial symmetry across hemispherical surfaces.

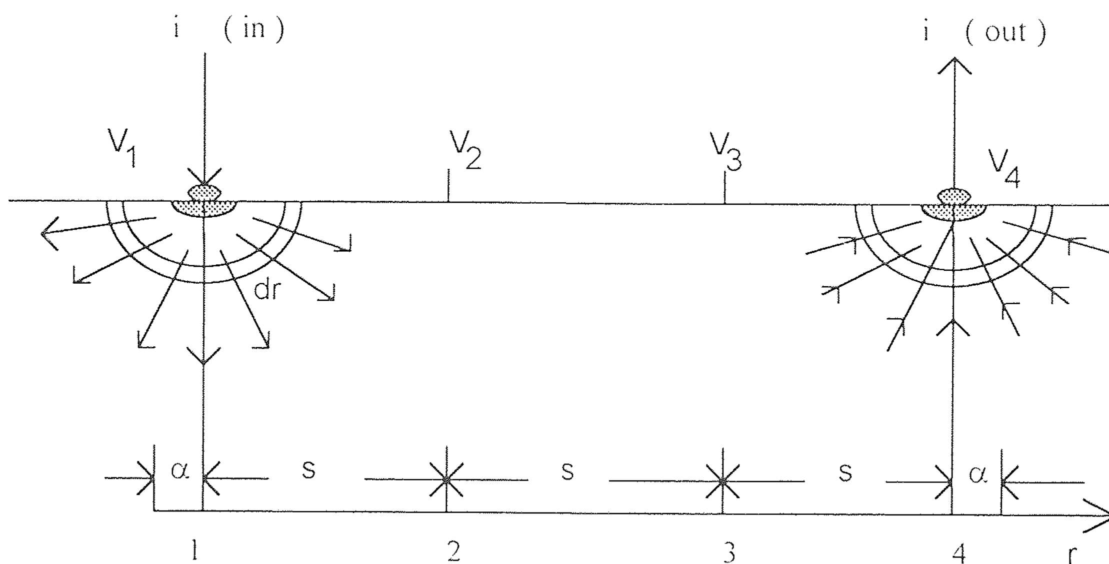

Figure 6 The figure used to derive the equation of four-probe measurement.

The potential difference between the probes 2 and 3 is $V=V_2 - V_3$, the relation between V and i is as follows

$$V_1 - V_2 = iR = i\int_{\alpha}^{s} \frac{\rho dr}{2\pi r^2} = i\rho(\frac{1}{2\pi\alpha} - \frac{1}{2\pi s}) \tag{2.29}$$

$$V_1 - V_3 = iR = i\int_{\alpha}^{2s} \frac{\rho dr}{2\pi r^2} = i\rho(\frac{1}{2\pi\alpha} - \frac{1}{2\pi 2s}) \tag{2.30}$$

$$(V_2 - V_3)_{1,in} = i\rho(\frac{1}{2\pi s} - \frac{1}{2\pi 2s}) = \frac{i\rho}{2\pi}(\frac{1}{s} - \frac{1}{2s}) \tag{2.31}$$

$$(V_2 - V_3)_{1,out} = i\rho(\frac{1}{2\pi s} - \frac{1}{2\pi 2s}) = \frac{i\rho}{2\pi}(\frac{1}{s} - \frac{1}{2s}) \tag{2.32}$$

$$V = V_2 - V_3 = (V_2 - V_3)_{1,in} + (V_2 - V_3)_{1,out} = \frac{i\rho}{2\pi s} \tag{2.33}$$

$$\rho = 2\pi s\,(V / i) \tag{2.34}$$

The specimen thickness is a significant parameter in the evaluation of the actual resistivity if the interprobe spacing, s, is comparable to the thickness, δ, shown in Fig. 3. In the limit, if the thickness $\delta << s$, the specimen may be considered as essentially two-dimensional, an infinite sheet having an infinitesimal thickness, δ. Since the current streamlines have radial symmetry in the homogenous isotropic sheet, Ohm's law is ($\partial V/\partial r$) = - $\rho\mathbf{J}$. The current density J and potential difference, V = V2 - V3, between probes 2 and 3 are, respectively,

$$J = \frac{i\,r}{2\pi\delta r} - \frac{i\,r'}{2\pi\delta r'}, \qquad V = -\rho\int_{2s}^{s} J dr \tag{2.35}$$

where the unit vectors r = - r' and r' = 3s - r; therefore,

$$V = \frac{i\rho}{2\pi\delta}\int_{s}^{2s}(\frac{1}{r} + \frac{1}{3s - r})dr \tag{2.36}$$

The solution of this integral then leads to the resistivity,

$$\rho = \frac{V}{i}\cdot\frac{\pi\delta}{\ln 2} = 4.5324\delta R \tag{2.37}$$

Equation (2.37) is adulate for determining the sheet resistivity, $\rho_s = \rho/\delta$, of an essentially infinite conducting sheet of infinitesimal thickness in comparison with the interprobe spacing, s.

A square four-probe array such as shown in Fig. 7 provides some advantages over a collinear array for measuring the resistivity of small area specimens. For a thin semi-infinite conducting sheet, $\delta \ll 0.5s$, measured by means of a square four-probe array the resistivity [14] is

$$\rho \cong 2\pi\delta R/\ln 2 \qquad (2.38)$$

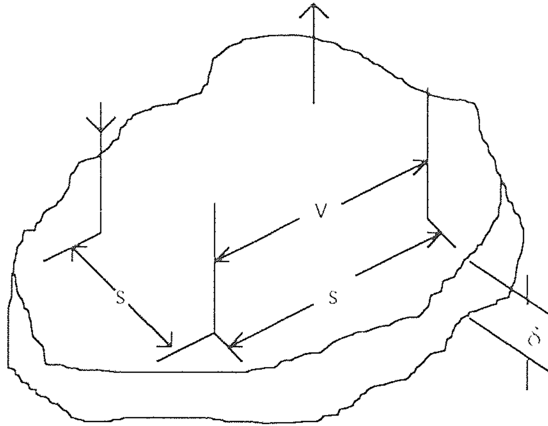

Figure 7 Square four-probe array on a semi-infinite surface of thickness, δ; current input and output points constitute current dipole; interprobe spacing is s.

For lamellae of an arbitrary shaped specimen, the equation for resistivity measurement uses the conformal representation developed by van der Pauw for mapping a specimen of arbitrary shape on a semi-infinite half-plane. This will be given in next section.

2.3 Van der Pauw theory

For measurements on lamellae of arbitrary shape whose contacts are on their periphery, the derivation of the basic equation is based on the conformal

representation developed by van der Pauw for mapping a specimen of arbitrary shape on a semi-infinite half-plane.[15]

Consider a continuous single-valued function of the form $z=f(t)=x(u,v)+jy(u,v)$ which defines a complex variable, $z=x+jy$ as a function of another variable $t=u+jv$. Let a particular value, t', represent a point in the complex plane of t. Then in the complex plane of z some particular value(or values), z', corresponds to t'. There is a similar correspondence for other points on the respective complex planes of t and z so that a curve on the t-plane is transformed by "conformal mapping" from the t-plane to the z-plane. Conformal mapping is an analytical technique used by van der Pauw to demonstrate a procedure for measuring the resistivity of a specimen having an arbitrary shape and thickness with four line electrodes on its periphery. Consider the semi-infinite plane of thickness, δ , shown in Fig.8 , line-electrodes

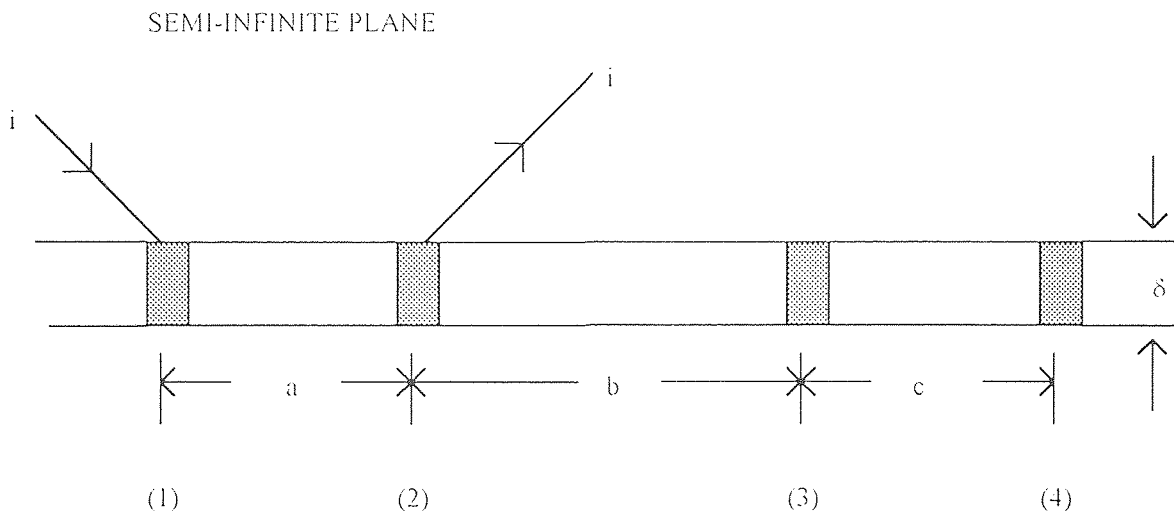

Figure 8 Representation of a semi-infinite half-plane of thickness, δ, with line-electrodes 1 and 2 for current terminals and 3 and 4 used for voltage probes.

1, 2, 3, and 4 on the plane boundary are separated from each other by the dimensions a, b, and c. Let a current , i , be introduced at electrode 1 and removed at electrode 2. It is assumed that the currents flowing out of and into the electrodes have radial symmetry across semi-circles. Therefore,

$$V_4 - V_3 = \left(-\frac{\rho\, i}{\pi\, \delta}\right) \int_{a+b}^{a+b+c} \frac{dr}{r} \qquad (2.39)$$

Solving the integral in Eq. (2.40) leads to

$$V_{3,4} = -\frac{\rho\, i}{\pi\, \delta}\, \ell n\left(\frac{a+b+c}{a+b}\right) \qquad (2.40)$$

The potential $V_{3,4}$ developed by the current , i , flowing out of the half-plane, between electrodes 3 and 4 is

$$V_{3,4} = \frac{\rho\, i}{\pi\, \delta} \int_{b}^{b+c} \frac{dr}{r} = \frac{\rho\, i}{\pi\, \delta}\, \ell n\left(\frac{b+c}{b}\right) \qquad (2.41)$$

The potential difference between Eqs.(2.41) and (2.42) is , therefore,

$$V_4 - V_3 = V_{3,4} = \frac{\rho\, i}{\pi\, \delta} \cdot \ell n \frac{(a+b)\ (b+c)}{b(a+b+c)} \qquad (2.42)$$

and the resistance determined from Eq.(2.43) is

$$R_{12,34} = \frac{V_{3,4}}{i} = \frac{\rho}{\pi \delta} \cdot \ell n \frac{(a+b)(b+c)}{b(a+b+c)} \qquad (2.43)$$

If the currents and voltage electrodes are commutated so that 2 and 3 are current electrodes and 1 and 4 are potential probes, then , solving the analog equations for the resistance lead to

$$R_{23,41} = \left(\frac{\rho}{\pi \delta}\right) \cdot \ell n\left[\frac{(b+c)(a+b)}{ac}\right] \qquad (2.44)$$

from Eqs.(2.44) and (2.45),

$$\exp\left[-\frac{\pi\delta}{\rho}R_{12,34}\right]+\exp\left[-\frac{\pi\delta}{\rho}R_{23,41}\right]=1 \tag{2.45}$$

Let $x_1 = \pi\delta R_{12,34}$ and $x_2 = \pi\delta R_{23,41}$; then expressing x_1 and x_2 in symmetric and anti-symmetric terms,

$$\frac{1}{2}=e^{-\left(\frac{x_1+x_2}{2\rho}\right)\cdot\cosh\left(\frac{x_1-x_2}{2\rho}\right)} \tag{2.46}$$

Now choose a function , f , so defined that

$$f=\left(\frac{2\rho}{x_1+x_2}\right)\cdot\ell n2 \tag{2.47}$$

then the resistivity, $\rho = (f/\ell n2)\,(x_1+x_2)/2$, is

$$\rho=\left(\frac{\pi\delta}{\ell n2}\right)\cdot\left(\frac{R_{12,34}+R_{23,41}}{2}\right)\cdot f \tag{2.48}$$

The function f can be evaluated by introducing Eq.(2.48) into (2.47)

$$\frac{R_{12,34}-R_{23,41}}{R_{12,34}+R_{23,41}}=\left(\frac{f}{\ell n2}\right)\cdot\text{arc cosh}\left[\frac{\exp(\ell n2/f)}{2}\right] \tag{2.49}$$

The function, f , on the right hand-side of this equation depends only on the ratio $R_{12,34} / R_{23,41}$ (i.e., on the commutated current and measured voltages.) Fig. 9 presents, in graphical form , the dependence of f on the ratio $R_{12,34} / R_{23,41}$. This curve has a maximum error of about 2 %. In order to average out some of the spurious emfs which can influence V_h , it is good to average over current and magnetic field polarities.

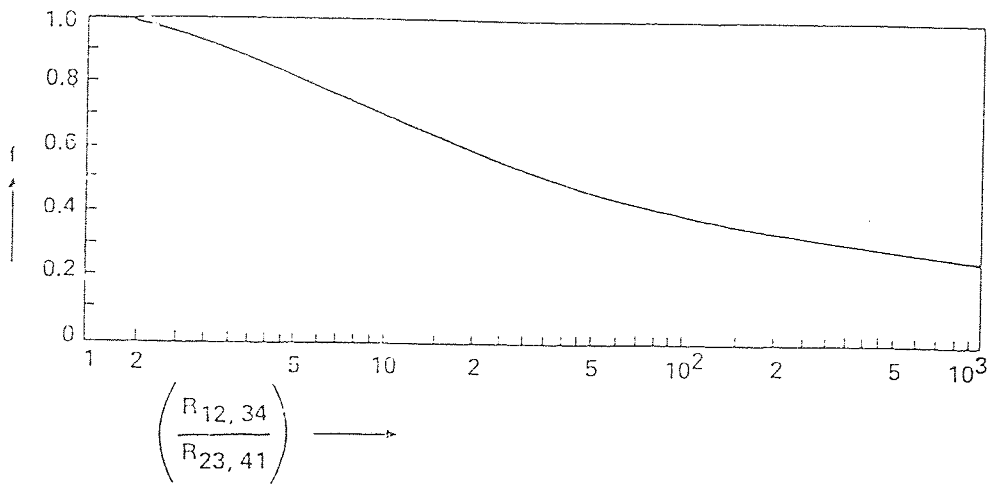

Figure 9 The function f used to determine the specific resistivity of a specimen with an arbitrary contour as a function of the resistance ratio $R_{12,34}/R_{23,41}$[15].

2.3 Systematic Errors

The calibration of the apparatus and fluctuations in experimentally measured parameters as well inherent or external noise sources limit the accuracy of Hall measurements. There are some specific errors of a systematic nature related to temperature gradients present in specimens subjected to Hall measurements . These have not been described in the earlier sections of this chapter in which the Hall effect is treated as an isothermal phenomenon without considering thermal or thermomagnetic effects. These are not described in detail in this thesis. If a longitudinal temperature gradient ∇T_x is present in a specimen then a transverse voltage V_n appears in it by virtue of the Ettingshausen-Nernst effect and also a transverse temperature gradient virtue of the Righi-Leduc effect. A transverse temperature gradient ∇T_y can generate a thermoelectric error voltage between the Hall electrodes if the specimen and its Hall contacts have a significant thermolectric power between them and if the thermoelectric power is itself a

significant function of the magnetic field. In most except ferromagnetic material the latter mechanism is usually of negligible significance.

A detailed theoretical treatment of thermomgnetic phenomena has been given by Jaggi [16]; adiabatic charge carrier transport has been treated in further detail in the monographs of Jan [17] and Beer [18]. Figure 8 shows some of the principal

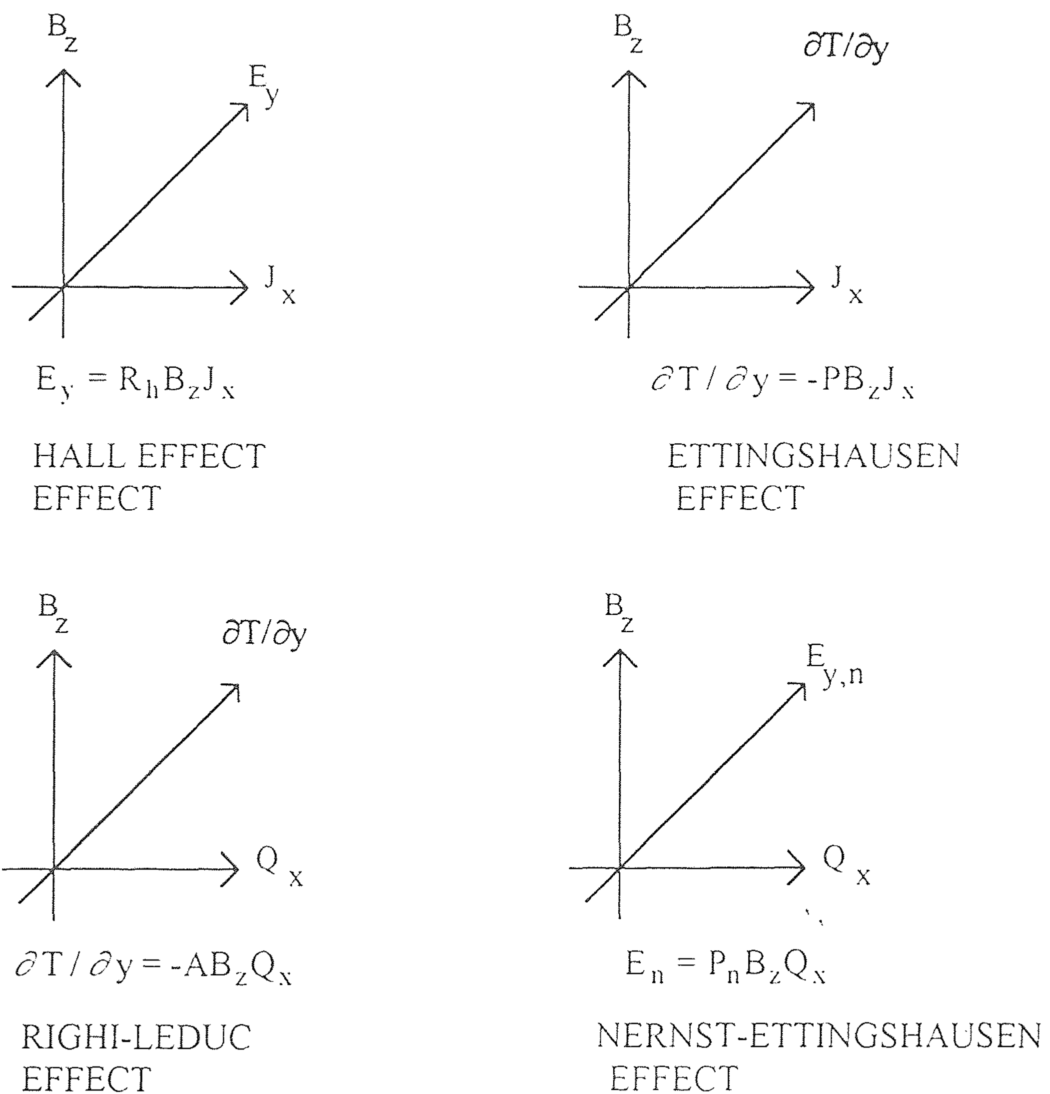

Figure 10 Hall effect and principal thermomagnetic effect shown with their their orientation in Cartesian coordinates. Q is the heat flux and $\partial T/\partial y$ is thermal gradient in the direction of Hall field.

thermomagnetic phenomena and their electrical, magnetic and thermal components. The Ettingshausen-Nernst and Righi-Leduc effects can be eliminated by preventing heat flow. However, the Ettingshausen effect is a function of electron flow in a magnetic field ; consequently, the transverse temperature gradient $\partial T/ \partial y$ is always present under usual experimental conditions and the Hall voltage is then adiabatic.

To avoid errors introduced by the Nernst-Ettingshausen and Righi-Leduc effects it is necessary to reduce or eliminate longitudinal heat flow such as may arise from localized Joule heating in an inhomogenous specimen from different amounts of heat transported along each of its current leads from the external environment and from the Peltier effect produced by differential thermoelectric heating of the junction between the current leads and the specimen. These effects can be reduced by providing a uniform thermal heat transfer, by thermal conduction to a heat sink, and by enclosing the specimen in a dewar thermostat in which a heat exchange gas such as helium is present. Such techniques have been described by Hurd [19] and by Alderson *et al.* [20]. It is not feasible, as a rule , to eliminate all of the thermomagnetic effects by choosing an appropriate specimen symmetry or by the control of its environment. The errors introduced by such thermomagnetic effects on Hall measurements can be eliminated by a permutation of the current polarity and magnetic field orientation will be described in later chapter. Let V_h be the true Hall voltage, V_0 the misalignment voltage, V_e the Ettingshausen voltage, V_r the Righi-Leduc voltage, Vn the Nernst-Ettingshausen voltage and ,V_t a thermoelectric error voltage generated by an externally imposed thermal gradient. Then Table 2.1 leads to

$$\frac{V_{m1} + V_{m4} - V_{m2} - V_{m3}}{4} = V_h + V_e = V_h + P\Pi \qquad (2.50)$$

where P is the Ettingshausen coefficient and Π is the thermoelectric power of the specimen.

In order to determine the Hall coefficient from such Hall measurements the thickness d of a wafer must be determined by means of mechanical probe measurements, by the use of a calibrated microscope equipped with a filar eyepiece, or a precision vernier caliper.

Table 2.1 Permutations of current and magnetic field for Hall measurement

mode	Potential measured between Hall terminals
B_+, i_+	$V_{m1} = V_h + V_o + V_e + V_T + V_N + V_r$
B_-, i_+	$V_{m2} = -V_h + V_o - V_e + V_T - V_N - V_r$
B_+, i_-	$V_{m3} = -V_h - V_o - V_e + V_T + V_N + V_r$
B_+, i_-	$V_{m4} = V_h - V_o + V_e + V_T - V_N - V_r$

A minor source of systematic error is the inhomogeneity of the magnet as shown by de Mey [21] using an in tegral equation technique. As a rough approximation he found that if the magnetic field has a homogeneity better than x% then the error in the Hall voltage is less than 0.5x%. Knoppe and Bryan [22] have considered an extreme case in which the magnetic field B, oriented as shown in Fig. 2 had a distribution, B(x), which decayed to half its peak value at a distance along the x-direction equal to half the width of the specimen; for such a case, the ratio of the Hall voltage V_{hi} to that measured in a homogenous magnetic field is

$V_{hi} / V_h \cong 0.8$. The fractional error in the value of the Hall coefficient can be expressed in terms of Eq. (2.8) in the form

$$\frac{\Delta R_h}{R_h} = \frac{\Delta V_h}{V_h} + \frac{\Delta d}{d} + \frac{\Delta i}{i} + \frac{\Delta B}{B} \quad (2.51)$$

For a specimen chosen to have the optimum thickness by means of Eq.(2.41) the fractional error in R_h is

$$\frac{\Delta R_h}{R_h} = \frac{\Delta i}{i} + \frac{\Delta B}{B} + 2\left(\frac{\Delta d \cdot \Delta V}{R_h iB}\right)^{\frac{1}{2}} \quad (2.52)$$

If the length of a rectangular wafer is not much greater than its width then a correction factor must be included in Eq.(2.8) to account for the reduction in Hall voltage produced by the electrostatic shorting of the field by the current electrodes. Various analytical techniques have been used to calculate the perturbation of the equipotentials and current streamlines in a rectangular plate produced as a function of its length to width , ℓ/w ratio, the extent of its contacts, and the Hall angle θ ,

$$V_h = R_h \cdot (Bi/d) \cdot F(\theta, \ell/w) \quad (2.53)$$

The geometrical correction factor, $F(\theta, \ell/w)$, is normalized in terms of V_h for $\ell/w \to \infty$. Results obtained experimentally and justified theoretically by Drabble *et al.* [23] indicate that it is possible to obtain Hall voltages comparable (within 5%) to rectangular specimens with $\ell/w >> 1$ provided that the metal contacts of specimens with $\ell/w < 1$ are replaced by a material whose resistivity is much larger than that of the specimens and that these contacts have lengths that are at least equal to their widths.

CHAPTER 3

EXPERIMENTAL PROCEDURES AND SET-UP HALL MEASUREMENT

3.1 Measurement Procedures

Hall effect measurements made on rectangular wafers such as shown in Fig. 2 require that the Hall voltage V_h be determined as a function of the magnetic field and DC input current in accordance with Eq.(2.8). the amplitude and polarity of V_h depends on the magnitude and polarity of i and on the direction of B relative to the coordinate axis. If terminal 1 is the positive polarity for a DC current i_+ and the direction of the steady-state magnetic field shown in Fig. 2 is defined as B_+ then the Hall voltage, measured between terminals 3 and 4 is such that terminal 3 is negative for an n-type material (dominant electronic conduction) and positive for a p-type material (dominant hole conduction). In an ideal situation these Hall electrodes are point contacts placed on an equipotential plane so that $V_h=0$ for $B=0$; in practice such conditions can be only approximated; in $B = 0$ there is usually a misalignment potential V_0 between them. The potential measured between the Hall electrodes for $B \neq 0$ is , therefore, the algebraic sum of the misalignment potential and of the Hall voltage, $V = V_h+V_0$. The misalignment potential can be eliminated by measuring V for two opposite orientation equal amplitude magnetic fields while keeping all other parameters constant.

If the current polarity and magnetic field orientations shown in Fig. 2 are indexed as i_+ and B_+, respectively, and the potential difference measured between the Hall electrodes is $V(B_+i_+)$, then for a permutation of polarities, the Hall coefficient can be described in terms of Eq. (2.8) as

$$R_h(C/cm^3) = \frac{2.5\times10^7 d}{|B|}\left[\frac{V(B_+,i_+)}{i_+} + \frac{V(B_+,i_-)}{i_-} - \frac{V(B_-,i_-)}{i_-} - \frac{V(B_-,i_+)}{i_+}\right] \quad (3.1)$$

The units of measurement usually encountered in practice and used in Eq.(3.1) are not a consistent set of units. They are compared in Table 3.1 against SI units.

Table 3.1 Units of measurement.

Quantity	SI units	Units for Hall coefficient measurements
resistivity, ρ	ohm-m	ohm-cm
charge carrier density, n, p	m^{-3}	cm^{-3}
mobility, μ	$m^2/V\text{-}sec$	$cm^2/V\text{-}sec$
Hall coefficient, R_h	m^3/C	cm^3/C
electric field	V/m	V/m
magnetic flux density, B	T	T or gauss
current density, J	A/m^2	A/cm^2
potential difference, V	V	V
physical dimensions, ρ,w, d	m	cm

Compensation of the misalignment voltage of Hall test structures may be desirable for high-resolution Hall measurements in particular for the case where the Hall voltage is an order of magnitude smaller than the uncompensated misalignment voltage. The compensation circuits shown in Fig. 11 provide a

temperature-independent compensation provided that the input current i_1 is constant, that the branch current $i_c << i_1$, and that $i_c = i_1(r_c/r)R_i$. Here the resistance r and r_c are indicated in Fig. 11 and the internal resistance R_i is that

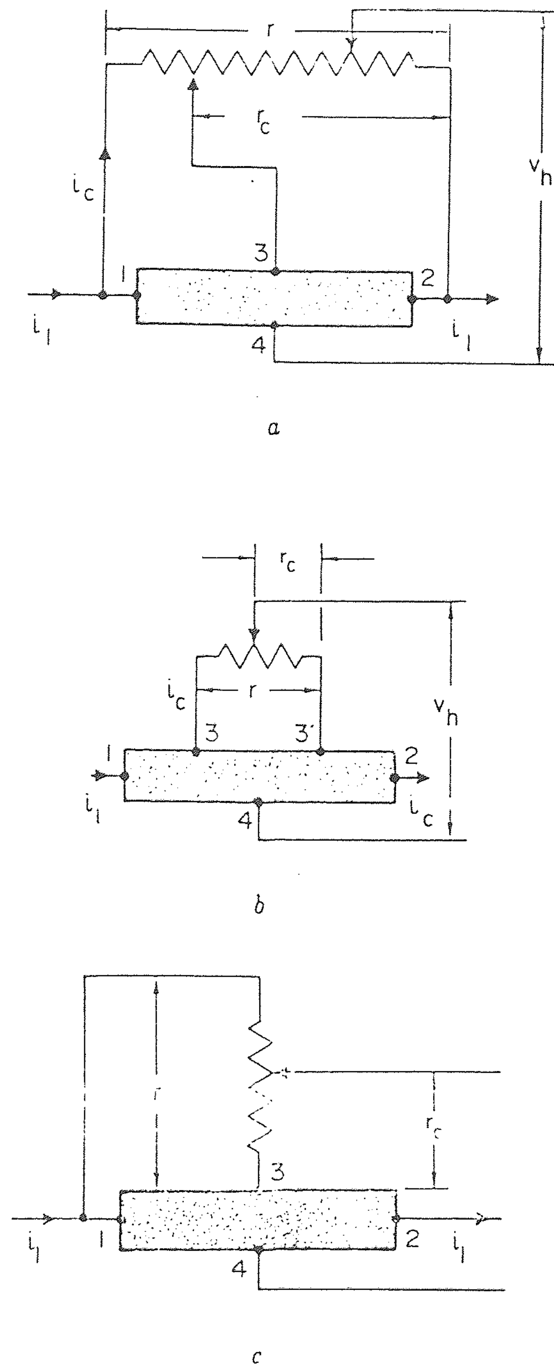

Figure 11 External compensation circuits for eliminating the misalignment potential between Hall electrodes.

present between contacts 1 and 2 for (a); between 3 and 3' for (b); and between 1 and 3 for (c). Only the compensation circuit shown in Fig. 11(b) is useful for large variations in magnetic field. The reason for this is that any magnetoresistance effects which influence R_i are the same as those which influence the test structure between contacts 1 and 2 at least to first order. For the other compensation schemes the misalignment voltage is itself a function of the magnetic field and , therefore, a potential source of magnetic field-dependent errors.

3.2 Van der Pauw Configuration

However, rather than a Hall-bar structure, it is probably more common to use one of the "van der Pauw" configurations , shown in Fig. 12. In this case, it is necessary to permute current (i,j) and voltage (k,l) leads in order to calculate ρ ,μ_h and n_h as follows

$$\rho = \frac{\pi d}{\ell n 2}\left[\frac{R_{21,34} + R_{32,41}}{2}\right] f \tag{3.2}$$

$$R_h = \frac{d}{B}\left[\frac{R_{31,42} + R_{42,13}}{2}\right] \tag{3.3}$$

where $R_{ij,k\ell} \equiv V_{k\ell} / I_{ij}$, and f should equal unity; if it does not, the material is probably inhomogeneous.

For the last more then 30 years, the van der Pauw technique has been one of the standard tools for measuring the resistivity, ρ, and the Hall coefficient, R_h, of materials. This measurement technique allows for the use of samples of arbitrary shape, unlike other methods like the bridge geometry, and also allows for a great

amount of freedom in the placement of the contact leads. Application of this technique, however, is contingent on four conditions: (a) The sample must be of a simply connected shape, (b) it must be laminar, (c) there must be four contact leads attached (at arbitrary positions) along the edge of the sample, and (d) these leads must be point-like in size. Among the other sample shapes that have been used experimentally are the square and the cloverleaf, shown along with the circle and Greek cross shape in Fig.12. The square is often the most convenient sample shape to fabricate. There are advantages and disadvantages to the various Hall-bar and van der Pauw configurations shown in Fig.12. Considerations such as these are discussed in detail in the book by Look [24] .

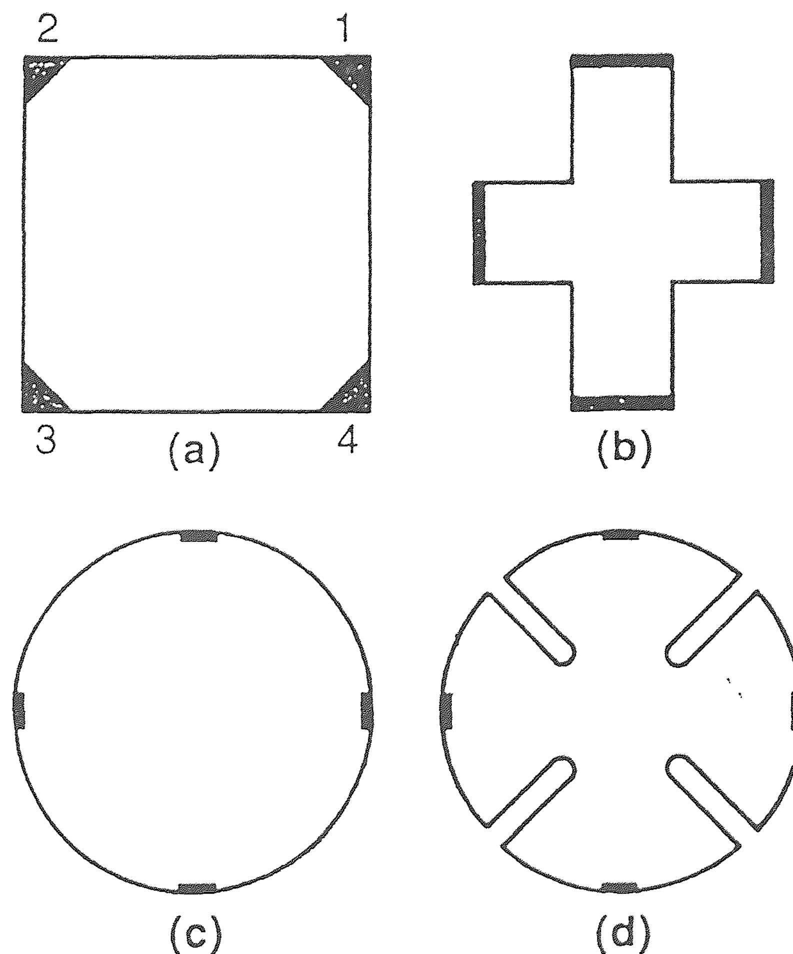

Figure 12 Four common patterns used for van der pauw resistivity and Hall effect: (a) Square (b) Greek cross (c) Circle (d) Cloverleaf.

3.3 Experimental Set-up of Hall Measurement

The essential components of apparatus for Hall effect measurements are: (a) a DC constant current source with provision for reversing its polarity; (b) an electrometer, galvanometer or high-impedance high-resolution digital or analog voltmeter with provision for reversal of its input polarity without affecting its accuracy or precision; (c) an electromagnet capable of providing an adjustable flux density from ~ 0.05 T to ~ 1.00 T with a homogeneity over the specimen volume of ± 1% and a precision and long-term stability of ±1%. A nuclear resonance magnetic field probe or a precision-calibrated Hall generator should be available to monitor the magnetic field between the magnet poles in the course of the measurements. Adequate provision should be made for reversing the direction of the magnetic field. If a permanent magnet is used to provide the magnetic field then provision should be made for rotating the specimen 180' about its axis parallel to the direction of current flow. In other respects the provisions and specifications for resistivity measurements described in Section of the Chapter 2.3 apply here as well.

If the Hall coefficient R_{h_1} determined on the first set of Hall electrodes differs by more than 10% from R_{h_2}, that determined on the second set of Hall electrodes, then the measurements should be discarded. They indicate an unacceptably large inhomogeneity. If the results are consistent to within 10% then the average Hall coefficient may be calculated from $\langle R_h \rangle = \frac{1}{2}(R_{h_1} + R_{h_2})$. Hall voltages are usually in the μv range. A high-sensitivity electrometer can be used as a microvolt detector and a differential amplifier interpolated between the Hall contacts and the electrometer allows both the specimen and the electrometer to be grounded. This reduces the residual common-mode error voltages across the electrometer.

3.4 Ohmic Contact

A variety of procedures have been used to make electrical contacts to specimens used for Hall effect measurements . In most cases the making of reliable ohmic contacts, particularly to large bandgap semiconductors, is an empirical art. The problem of contact resistance encountered with pressure-type contacts can lead to large random errors of measurement. Pressure contacts are common for routine room temperature measurements on metals and on narrow bandgap semiconductors. Pressure contacts are also used for high temperature Hall measurements, however, at low temperature they tend to develop large contact resistance. Metallic points of tungsten or tungsten alloys are often used as pressure contacts; for high temperature applications or reactive materials graphite is used for pressure contacts.

Soldered contacts using indium or low temperature indium eutectic alloys can be used for making reliable contacts to low temperature bandgap semiconductors such as InSb or InAs. The soldering should preferably be done in an oxygen-free environment in order to prevent the formation of a "cold-solder joint". Painted contacts made of a metallic powder such as silver or gold in a colloidal organic binder are used for rudimentary contacts on small bandgap semiconductors. Electroplated or electroless-plated contacts of copper, gold, or rhodium should be used with caution because they tend to have high and randomly variable contact resistances at low temperatures.

A review of the basic theory of ohmic contacts and of their specific technology relevant to III-V compound semiconductors has been given by Rideout [25]. He concludes that for the larger bandgap semiconducting compounds no material exists with low enough work function which might yield a low contact barrier . Alloy regrowth, in-diffusion of a dopant contained in the specimen, epitaxial growth of a more heavily doped n- or p-layer, or ion implantation are

promising techniques for the formation of ohmic contacts. Table 3.2 presents a selection of his collected data with particular emphasis on Hall effect measurements.

Table 3.2 Ohmic contact technology for III-V conpound semiconductors.

Compound	Conductivity type	Contact material	Deposition technique	Alloying temp. , °C
$A\ell P$	n	Ga-Ag	Perform	150
$A\ell As$	n, p	In-Te	Preform	160
$A\ell As$	n, p	Au	Preform	700
	n, p	Au-Ge	Preform	
	n	Au-Sn	Preform	
GaAs	n	Au-Ge(88:12)	evap.	350-450
	n	Au-Te(98:2)	evap.	500
	n	Au-Si(94:6)	evap.	300
InP	n	Ag-Sn	Preform evap.	600
InAs	n	In	Preform	
	n	Sn-Te(99:1)	Preform	
InSb	n	In	Preform	
	n	Sn-Te(99:1)	Preform	

CHAPTER 4

HALL MEASUREMENT RESULT AND CONCLUSIONS`

4.1 Equipment System of Hall measurement

The experimental Hall measurement system included the following equipment: (a) an electromagnet with power supply to provide the B field . we use V--4005 Four-inch Electromagnet with V-2900/V-FR2900 power supplies. (b) a device to measure the B field .we use the Model 620 Pre-Calibrated Hall Effect Gaussmeter. (c) a voltmeter to measure the Hall voltage. we use the 195A Digital Multimeter. (d) a DC source to provide the current I. we use the Programmable Regatron. (e) an ammeter to measure the current I. we use a Model 3020 Digital Mulitimeter. The range and precision of the equipment show in the table 4.1.

Table 4.1 The range and precision of the equipment

Equipment	Range	Precision
Electromagnet (V-4005 Four-inch)	0.165 k gauss-4.62 k gauss	± 5 gauss
Power supplies (V-2900)	1 A - 65 A	± 1 A
Gauss meter (Model 620)	0.1 -30 k gauss	±0.5% FS to 10 kG ±1% to 30 kg
Digital Multimeter V	1mV -200V	±0.5mV

(195A DIGITAL MULITMETER)		
DC source (Programmable Regatron)	0 - 100mA	±0.5mA
Digital Multimeter, I (Modle 3020)	200μA -2mA	±0.5 μA

4.2 Experiment of Hall Effect

As we already mentioned in chapter 2, to determine the Hall mobility μ_h, we must also perform a conductivity experiment. We set up a system using the van der Pauw method that can determine the Hall coefficient, R_h, and resistivity, ρ, in one experiment. Two samples 1.5-μm-thick epilayers were used to examine and study the Hall effect-type van der Pauw system and measurement . Both were made in samples the shape of a square ($7\times7mm^2$) for convenience to fabricate. One of the samples is GaAs epilayer on semi-insulating (SI) GaAs substrate with impurity N_b=-2.12×10^{15} cm^{-3} and Ns=$-3.18\times10^{11}cm^{-2}$. This sample is a standard sample to examine the experimental system. The other sample is $In_xGa_{1-x}As$ on SI GaAs grown by MBE. The results are shown in the Table 4.2. We used Eq. (3.1) to get $x=\frac{R_1+R_2}{2}$, $R_1=V_1/I$,$R_2=V_2/I$, and f is a factor due to shape asymmetry. To get f(x) we used Eq.(2.47) . For all the structures in Fig.12, f should equal unity. So,

From Eq.(3.2) $\rho=\frac{\pi d}{\ell n2}\left[\frac{R_{21,34}+R_{32,41}}{2}\right]f$ and Eq.(2.28)

Table 4.2 Experiment result of the sample (GaAs/GaAs)

B (kG)	I (A)	d (μm)	V_h (mV)	R_h (cm^3/C)	V_1 (mV)	V_2 (mV)	R_1 (Ohm)	R_2 (Ohm)	x	f(x)
1.45	100μ	1.5	-29.75	3077	197.5	92.75	1975	927.5	2.13	0.9547
2.5	100μ	1.5	-53.75	3225	197.75	92.5	1977.5	925	2.14	0.9547

$n_h = 6.25 \times 10^{10} \dfrac{I(amp)B(gauss)}{V_h(volts)d(cm)} cm^{-3}$, we can get resistivity ρ and n_h, and also get $\mu_h = R_h \sigma$. In sample 2 no mobility and Hall voltage could be measured at 300 K with x=0.5 since the resistivity was too high.

4.3 Result and Discussion

The comparison of sampling and standard Hall measurement is shown in Table 4.2.

Table 4.2 Comparison of sampling and standard Hall measurement

	μ_h (cm^2/V-s)	n (cm^{-3})	ρ (ohm-cm)
Standard	3339	2.12×10^{15}	0.88154
Sampling	3347	1.98×10^{15}	0.9414

Table 4.2 displays an example of typical result we observed at 300 K for an n-type sample of GaAs while monitoring the Hall mobility μ_h and the concentration n values. Care was taken to check the variation in resistivity and the Hall

coefficient with magnetic field. Two methods were used. In the first, resistivity and the Hall coefficient were measured for field of 1-6 kG. The measurements were performed at zero field, with an applied, and again at zero field. In the second, field spanning the range 1-6 kG were selected and the order in which the field measurements were performed was decided by a table of random numbers. In this way any effects associated with increasing or decreasing magnetic field were avoided. In both approaches, no variation with the magnetic field were observed, so that Hall coefficient sign changes caused by magnetic effects were eliminated.

Combined with increased computerization and use of digital instruments researches now demand even more performance from their equipment. For making transport measurements, as an example, an awareness of quantization errors is critically important. It is not claimed here that such errors can be completely eliminated or that the accuracy of these measurements is easily improved by 2 or 3 orders of magnitude. However, it is shown that careful attention to the limitations of the experimental systems and use of simple techniques such as the averaging procedure introduced can be very effective in improving measurement results.

CHAPTER 5

CONCLUSIONS

In conclusion, it has been shown that the van der Pauw-type Hall effect measurement is a useful tool in the electrical characterization of semiconductor materials . We set up the Hall effect measurement system and examined the system with a standard sample . The experimental results show that this Hall measurement system worked as well as expected. We also used this system to study the InGaAs/GaAs grown by MBE. Later we will set up the temperature-dependent van der Pauw measurement system which is more useful to study the material of semiconductor.

REFERENCES

1 E. H. Hall, *Amer. J. Math.*, 2 (1879), 287

2 H. Sakaki, L. L. Chang, R. Ludeke, C. Chang, G. A. Halasz, and L.Esaki, *Appl. Phys. Lett.* 31, 211(1977)

3 W. Dobblelaere, W. De Raedt, J. De Boeck, R.Mertens, and G. Borghs, *Electron. Lett.* 28, 372(1992)

4 K. J. Kuhn and R. B. Darling, *IEEE Trans. Electron Devices* ED-39, 1288(1992)

5 R. A. A. Kubiak, E.H.C. Parker, and S.Newstead, *Appl. Phys.* A35, 61(1984)

6 K.R. Breen, P. N. Uppal, and J. S. Ahearn, *J. Vac. Sci. Technol.* B 7, 758(1989)

7 G. L. Price, *Appl. Phys. Lett.* 53, 1288(1988)

8 M. J. Ekenstedt, P. Songpongs, and T. G. Andersson, *Appl. Phys. Lett.* 61, 789(1992)

9 B. J. Baliga and S. K. Ghandhi, *J. Electrochem. Soc.* 122, 683(1975)

10 S. Fujita, Y Nakaoka, T. Uemura, M. Tabuchi, S. Noda, Y. Takeda, and A. Sasaki, *J. Cryst. Growth* 95, 224(1989)

11 A. R. Billings, *Tensor Properties of Materials*, Wiley Interscience, London (1969)78.

12 R . G . Chambers, *Proc. Soc.* (London), A65(1952)903.

13 C. Hilsum and A. C. Rose-Innes, *Semiconducting I I I-V Compounds,* Pergamon Press, Oxford(1961)120.

14 A. Uhlir, Jr., *Bell Syst. Tech. J.* , 34(1955)105.

15 L. J. van der Pauw, *Philips Res. Repts.* , 13(1958)1.

16 R. Jaggi, *The Galvanomagnetic and Thermomagnetic Transverse Effects in "Zahlenwerte and Functionen,"* K. H. Hellwege and A. M. Hellewege, ed., Berlin(1959)161.

17 J. P. Jan, *Solid State Phys.*, 5(1957)1.

18 A. C. Beer, Galvanomagnetic Effects in Semiconductors, *Solid State Phys. Suppl. 4*, Academic Press, New York(1963)344.

19 C. M. Hurd, *J. Sci. Instr.*, 42(1965)465.

20 J. E. A. Alderson, T. Farrell and C. M. Hurd, *Phys. Rev.*, 174(1968)729.

21 G. de Mey, *Solid-State Electron.*, 20(1977)139.

22 H. Koppe and J. M. Bryan, *Can. J. Phys.*, 29(1951)274.

23 J. R. Drabble, M. M. Kaila and H. J. Goldsmid, *J. Phys. D, Appl. Phys.*, 8(1975)790.

24 D. C. Look, "*Electrical Characterization of GaAs Materials and Devices,*" John Wiley & Sons, New York(1989).

25 V. L. Rideout, *Solid-State Electron.*, 18(1975)541.